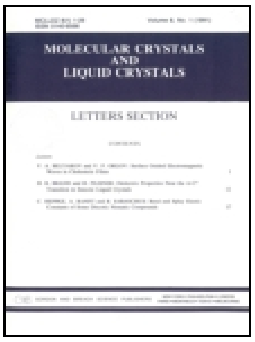

Molecular Crystals and Liquid Crystals

ISSN: 1542-1406 (Print) 1563-5287 (Online) Journal homepage: http://www.tandfonline.com/loi/gmcl20

Dielectric Study of Liquid Crystals with Large Electroclinic Effect

O. E. Panarina, Yu. P. Panarin & J. K. Vij

To cite this article: O. E. Panarina, Yu. P. Panarin & J. K. Vij (2015) Dielectric Study of Liquid Crystals with Large Electroclinic Effect, Molecular Crystals and Liquid Crystals, 610:1, 193-200, DOI: 10.1080/15421406.2015.1025650

To link to this article: http://dx.doi.org/10.1080/15421406.2015.1025650

Mol. Cryst. Liq. Cryst., Vol. 610: pp. 193–200, 2015
Copyright © Taylor & Francis Group, LLC
ISSN: 1542-1406 print/1563-5287 online
DOI: 10.1080/15421406.2015.1025650

Dielectric Study of Liquid Crystals with Large Electroclinic Effect

O. E. PANARINA,[1] YU. P. PANARIN,[1,2,*] AND J. K. VIJ[1,*]

[1]Advanced Materials Laboratory Department of Electronic and Electrical Engineering, Trinity College, University of Dublin, Dublin, Ireland
[2]School of Electrical & Electronic Engineering, Dublin Institute of Technology, Dublin, Ireland

*Here we report results of the study of tilt angle and birefringence of some "high-electroclinic" materials having similar molecular structure with two and three siloxane spacers. The structure of these LC materials were studied by dielectric spectroscopy, birefringence and tilt angle measurements. Three of the four studied materials with a siloxane fragment are the deVries materials, but the siloxane-free sample is conventional Sm*A *phase and is thus different. Possible models for the molecular structures of deVries Sm*A* phases are discussed.*

Keywords deVries liquid crystal; electroclinic effect; dielectric relaxation; electro-optic effects

Introduction

It is well known that the smectic layer spacing in the tilted smectic phases is lower than in the orthogonal smectic phases due to the molecular tilt. Nevertheless, in 1972, Diele *et al.* [1] reported a Sm*A* phase, with the same layer spacing as a non-chiral Sm*C*. Somewhat later, the unusual Sm*A*-Sm*C* phase transition without the smectic layer shrinkage was observed in several publications both in the non-chiral [2–4] and recently in the chiral smectic LCs [5–9].

To explain the nature of the Sm*A*-Sm*C* transition without alteration in the smectic layer spacing, deVries in 1974 suggested [2] a new type of Sm*A* phase, where the molecules are tilted similar to those in the Sm*C* phase. In one possible structure the tilted Sm*C*-like smectic layers "are stacked in a random fashion" [3]. In other words, the molecules are tilted with respect to the smectic layer normal, similar to those in the Sm*C* phase but the tilt directions in different smectic layers are randomly oriented or, strictly speaking, there is no long-range correlations in azimuthal angle of the smectic layers. In this phase the local symmetry of the smectic layer (C_{2h}) is the same as for the Sm*C* and in the case of chiral molecules the smectic layers possess the local spontaneous polarization. The overall

---

*Address correspondence to Yu. P. Panarin and J. K. Vij, Advanced Materials Laboratory Department of Electronic and Electrical Engineering, Trinity College, University of Dublin, Dublin 2, Ireland. E-mail: yuri.panarin@dit.ie; jvij@tcd.ie

Color versions of one or more of the figures in the article can be found online at www.tandfonline.com/gmcl.

symmetry of such a structure is $D_{\infty h}$, due to an averaging on all smectic layers and is the same as in conventional orthogonal Sm*A* phase.

Later on, deVries suggested another possible structure, the so-called "diffuse-cone" model, where the molecules are tilted but there is no long-range order in the azimuthal angle within each smectic layer and only short-range correlation in the tilting sense [4]. Hence, due to the averaging on any smectic layer, the uniaxial symmetry of Sm*A* phase is observed. The overall symmetry of this arrangement as well as the local symmetry is $D_{\infty h}$, as of a conventional orthogonal Sm*A* phase.

For the case of non-chiral liquid crystalline molecules, due to the absence of local spontaneous polarization, both possible structures cannot be optically distinguished from each other and from the orthogonal Sm*A* phase. Nevertheless the suggested deVries phase was supported by the [5] Raman spectroscopic study enables a determination of the order parameters <P2> and <P4> and has found the tilt angle as 32° for the TSiKN65 material.

The behavior of this type of SmA^* materials under the application of the external electric field was found to be different from the orthogonal SmA^*, namely very large electroclinic effect and a manner in which the saturation of the induced tilt angle with voltage is achieved. Both features can be explained by diffuse-cone model. The macroscopic behavior of the materials with the field-induced SmA^*-SmC^* phase transition was initially explained by a large high-order coefficient (Θ^6) in the Landau free-energy expansion [6, 7]. This explanation may probably be correct for some previously studied materials, but contradicts to the experimental [8, 9] studies of low molecular weight organosiloxane compounds where the dichroic ratio and the birefringence are considerably lower than in the field-unwound SmC^* phase and these show pronounced voltage dependencies.

The two properties: the unshrinkable smectic layers at the SmA^*-SmC^* transition and a large electroclinic coefficient appear to be the essential features of the deVries materials, though differing explanations for these effects have been given. The deVries materials exhibit a pronounced electroclinic effect due to the existence of a large molecular tilt in the Sm*A* phase. There is, however an alternative model where a large electroclinic effect [10–11] can be expected in materials in structure similar to the conventional Sm*A* but with a low orientational order parameter and a highly condensed smectic density wave. This model also explains the weak layer contraction. Theoretical models [12–14] predict the nature of Sm*A* to Sm*C* (*A to C*) transition in deVries smectics to be near the tricritical point. These two models give opposite results for the molecular orientational distribution function (ODF). Accordingly for the diffuse-cone model, the maximal probability density reaches the cone angle θ (the so-called volcano distribution) while the second approach gives a maximum probability density in a direction parallel to the smectic layer normal (sugar loaf). Although diffuse-cone distribution is unambiguously confirmed by the Raman study [5], this does not reject that Sm*A* materials (rather than Vries) may possess large electroclinic coefficient. Strictly speaking, the molecules in conventional Sm*A* phase are not perfectly perpendicular to the smectic layer either due to the non-ideal molecular shape or the thermal fluctuations. Nevertheless, the average molecular director is perpendicular to the layers plane. In deVries phase however the local director of a sufficiently large volume (within the coherence length, ξ) makes a non-zero angle θ with the smectic layer normal. Monte-Carlo simulations of molecular ordering in liquid crystals composed of bent-rod strongly angled molecules with siloxane end segment [15] showed that both mechanisms for electroclinic effect may exist at the same time.

In this paper we present the results of the optical and dielectric spectroscopy study of three different liquid crystal samples with siloxane end segment possessing the deVries type of SmA^* phases. The experimental results for these materials are compared with a

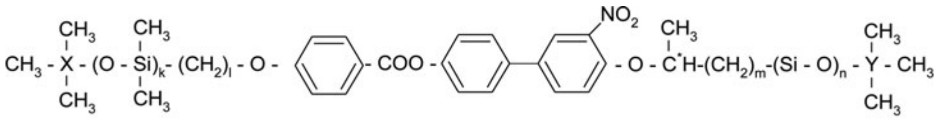

Component	Phase transitions	X	k	l	m	n	Y
DSiKN65	SmC* - 39 °C – SmA – 55 °C – Is	Si	1	6	4	0	C
TSiKN65	SmC* - 25 °C – SmA – 56 °C – Is	Si	2	6	4	0	C
12KN5DSi	SmC* - 42 °C – SmA – 59 °C - Is	C	0	11	4	1	Si
125KN	SmC* - 33 °C – SmA – 78 °C – Is	C	0	11	4	0	C

Figure 1. The molecular structure and the phase transition temperatures of the four studied samples.

similar compound but without siloxane segment in order to understand the nature and the structural arrangement of these phases. We conclude that both types of the molecular structures suggested by deVries [2–4] are possible and both of them are observed in the present work.

Experimental

We have investigated four different low molecular weight so-called electroclinic liquid crystals with closely related chemical structures: DSiKN65, TSiKN65, 12KN5DSi, and KN125. These materials were synthesized in Prof. Shashidhar Laboratory in Washington [16–18]. Their molecular structures along with the transition temperatures are shown in Fig. 1

All the studied materials have similar structures (or a similar structure) with the same core and exhibit high electroclinic effect with large induced tilt angle. The first three compounds have an organosiloxane fragments while the last one, 125KN does not. There is also a difference in the electro-optic and dielectric behavior between 125KN compound and the other three and this will be discussed later on.

Results and Discussion

The cells for electro-optic measurements were made with two ITO glasses coated with Nissan 1266 polymer. The polymer layer was rubbed in order to get homogeneous planar alignment. The cell thickness was about 9 μm. The cells were filled with the LC in its isotropic state and then cooled down slowly to the SmA^* phase. An AC electric field (20 Hz) was applied on the sample during the cooling process in order to train LC molecules and to achieve better alignment. Then the cell was placed in a hot-stage controlled by Eurotherm-2604 with accuracy of 0.01°C.

Induced Tilt Angle Measurements

The tilt angles in the SmA^* were measured by applying a low frequency electric field and rotating the sample in the polarizing microscope to the dark state. The electrically induced optical tilt angle is measured as a function of the applied voltage for different temperatures. The dependence of the induced angles for all the four studied components were more or less

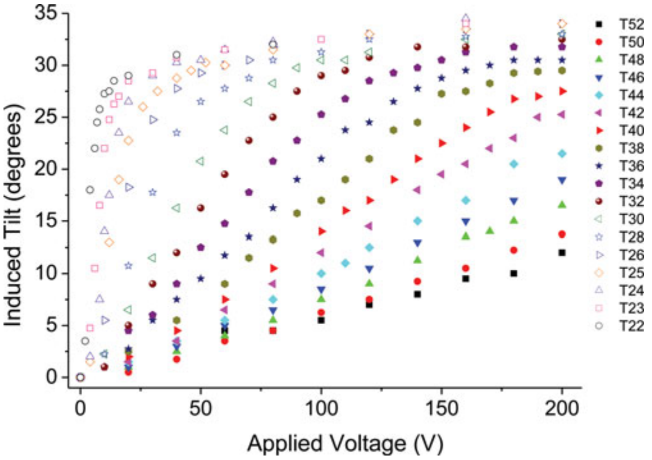

Figure 2. The dependence of the induced angles for 9 μm cell TSiKN65 for different temperatures.

similar to TSiKN65, which is shown in the Fig. 2. For temperatures close to the transition to isotropic phase the dependence is linear which is typical for the conventional electroclinic effect, but as the sample approaches phase transition temperature, the shape of the curves changes. With an increase in the applied voltage, the dependence becomes non-linear; tilt angle saturates at a value of about 32–33°. The response of the tilt angle to the external electric field shows Langevin-type dependence. For all the four materials the saturated voltage is considerably large and decreases rapidly on cooling, while the saturation angle stays almost the same.

Nevertheless, there is an essential difference in the electric field behavior of birefringence with electric field. In the siloxane contained samples, the birefringence increases with applied field, while in siloxane-free KN125 it remains almost constant with the field. The first scenario is typical of the diffuse-cone model while the second one is valid for the rigid core model.

The electrically induced angle obtained in this way is referred to as apparent tilt angle (θ_a) and is due to both the electroclinic effect (electric field-induction of the tilt angle for chiral molecules) and the diffuse-cone angle θ_0. [15]. Therefore the apparent tilt angle is the sum of both angles:

$$\theta_\alpha + \theta_0 + \theta e \tag{1}$$

Where, θ_0 is the diffuse-cone tilt (deVries) angle in the absence of electric field and θ_e is electrically induced (electroclinic) tilt angle according to the rigid-core model.

The value of the diffuse-cone tilt (θ_0) angle can be obtained from different techniques such as: from <P4> parameter (Raman spectroscopy [5]); smectic layer thickness (X-Ray [1–4, 16, 19]), free-standing film thickness [20, 21], birefringence [9, 17, and 22] and dielectric spectroscopy [23]. In this paper we have employed the last two techniques.

Dielectric Spectroscopy

Dielectric spectroscopy is a useful complementary technique to birefringence, x-rays for characterizing different phases and for finding structures in the various LC phases such as the AFLC [24], de Vries [25, 26], TGBA [23], etc... Here we use this technique to

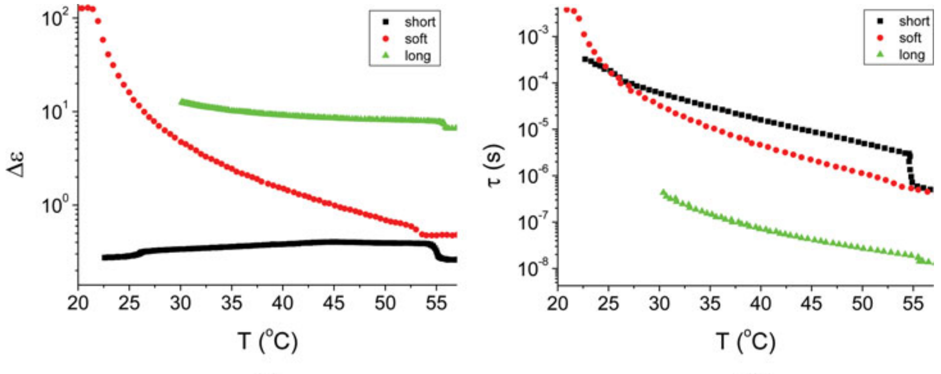

(a) (b)

Figure 3. The temperature dependence of dielectric strength $\Delta\varepsilon$ (a) and relaxation time, τ (b) for three relaxation processes observed in: homeotropic cell- molecular relaxation process around short molecular axis (■); and in planar cell–soft mode (●) and molecular relaxation process around long molecular axis (▲).

estimate the angle between the long molecular axis and the electric field and thus determine the diffuse-cone angle.

Dielectric measurements in the frequency range 1 Hz to 10 MHz were made using the Alpha-A impedance analyzer (Novocontrol) in the frequency range 1 MHz to 1 GHz using Agilent 4291B impedance analyzer.

For dielectric measurements, two cells (homeotropic and planar) each of cell thickness 15 μm were prepared, the Mylar thin-film stripes were used as spacers. The homeotropic cells consisted of two glass plates with ITO (Indium Tin Oxide) layers with relatively low resistance of 30 $\sigma/\square$ as electrodes. The substrates were coated with carboxylato chromium complex (chromolane) films for homeotropic alignment. The textures of the phases and the performance of alignment were checked using polarizing microscope.

The planar (homogeneous) cells made from brass coin electrodes to reduce a parasitic effect (peak) arising from a non-zero ITO layer resistance. Both electrodes were coated by polyimide films (RN-1175, Nissan Chemical Industry) to achieve the planar alignment. The polymer layers on two substrates were rubbed in the same direction after curing for the duration of 1h at a temperature of 250°C. The cells were placed in a hot-stage and interfaced to a Novocontrol Quatro Cryo-system temperature controller with a temperature accuracy of 0.01°C.

Three relaxation processes are observed in all the studied materials. Only one relaxation process was observed in a homeotropic cell and this is molecular process around the short molecular axis. Two relaxation processes were observed in planar cells: the lower frequency relaxation process is a soft mode and the higher frequency one is molecular relaxation process around the short molecular axis. The temperature dependence of dielectric strength $\Delta\varepsilon$ (a) and relaxation times, τ (b) for three relaxation processes are shown in the Fig. 3 as an example for TSiKN65.

All curves have a negative slop with temperature except for the dielectric strength of molecular relaxation process around the short molecular axis, which has a different behavior in different samples and is presented separately in Fig. 4 This will be discussed later on.

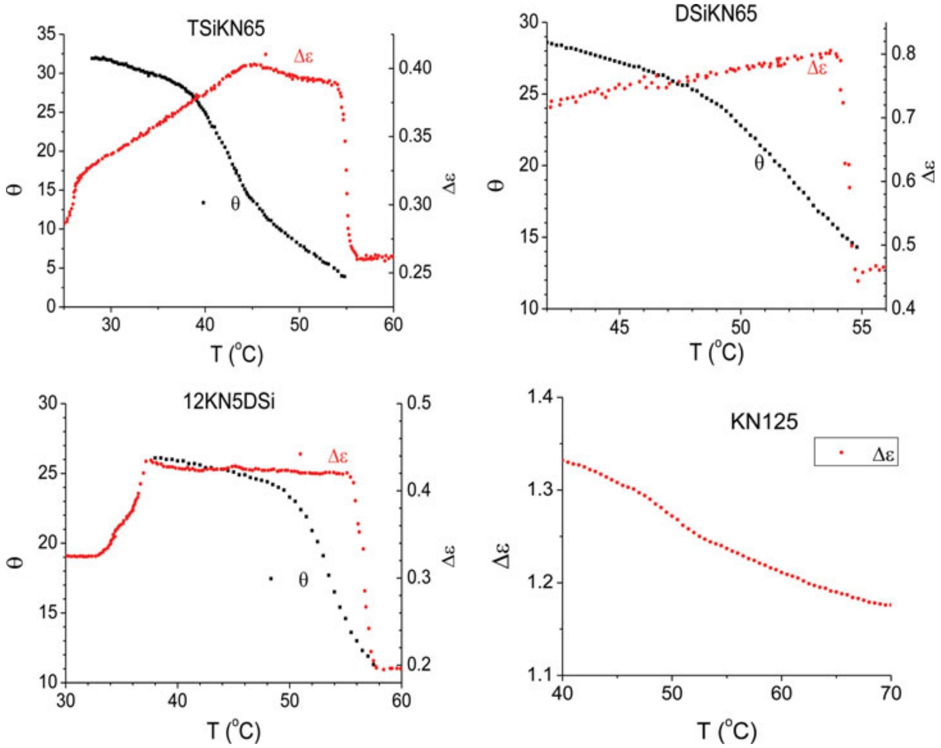

Figure 4. The temperature dependence of diffuse-cone angle, θ_0 and dielectric strength $\Delta\varepsilon$ of molecular relaxation process around short molecular axis.

Birefringence Measurements

As mentioned before in the siloxane-contained samples the birefringence increases with the applied field (see Fig. 5) while in KN125 it remains almost constant with field. The first scenario is typical for diffuse-cone model while the second one is valid for rigid core model.

The change in the effective birefringence can be used to determine the molecular tilt angle in undistorted (uniaxial) deVries Sm*A* phase. In the absence of electric field the


0 V 40 V 100 V

Figure 5. The textures (colors) of TSiKN65 9 μm cell for different applied voltages measured at T = 30°C.

effective birefringence of the deVries phase (Δn_{eff}) is always lower than the birefringence of a completely unwound field-induced Sm*C* structure (Δn_0). The value of diffuse-cone angle can be calculated from the following expression:

$$\theta_0 = \sin^{-1}\sqrt{\frac{2}{3}\left(1 - \frac{\Delta n_{eff}}{\Delta n_0}\right)} \tag{2}$$

The temperature dependencies of the diffuse-cone angle calculated from the birefringence measurements are presented in Fig.4.

Discussion

A total of three relaxation processes are observed in the dielectric spectra of the studied materials: two molecular relaxation processes around the short and the long molecular axes respectively and the soft mode. The temperature dependence of the dielectric strength of the molecular relaxation process usually shows a negative slop and furthermore it follows the Arrhenius law and this is valid for siloxane-free 125KN (see Fig. 4). This is true for relaxation process around the long molecular axis but is not valid for the relaxation process around the short axis for materials with siloxane fragments (Figs. 3(a) and 4). This can be explained by non-zero and temperature dependent diffuse–cone angle. The dielectric strength of the molecular relaxation processes around the short axis is proportional to the angle between the long molecular axis and the electric field which for the diffuse–cone angle depends on the factor $cos^2(\theta)$. Therefore for deVries materials the diffuse–cone angle increases on cooling. This causes a decrease in the dielectric strength and this opposes the Arrhenius slope, E_a/k_B, where E_a is the activation energy. Therefore the temperature dependence of the dielectric strength may decrease on cooling if $cos^2(\theta(T))$ exceeds the Arrhenius tendency. This is the case of DSiKN65 (Fig. 4). In 12KN5DSi dielectric strength is almost independent of temperature due to a compensation of the opposite trends. In TSiKN65 with largest diffuse–cone angle among the studied materials the dielectric strength initially grows on cooling and then begins to drop. This unexpected behavior can be explained by the fact that molecular shape is strongly non-calamitic due to a large siloxane fragment. This will be studied in future.

Conclusion

Four "high-electroclinic" materials having similar molecular structures were studied by dielectric spectroscopy, birefringence and the tilt angle measurements. Three of the four studied materials with a siloxane fragment are deVries materials, but the siloxane-free sample has a conventional Sm*A* phase. Therefore, the siloxane tail is responsible for the deVries structure due to the formation of a strongly non-calamitic bent molecular shape.

Funding

We thank the Science Foundation of Ireland for the grant 13/US/I2866 under Ireland-US co-operative research program.

References

[1] Diele, S., Brand, P., & Sackmann, H. (1972). *Mol. Cryst. Liq. Cryst.*, *16*, 105.

[2] De Vries, A. (1974). Abstracts Book of 5th International Liquid Crystal Conference, 150, Stockholm.

[3] De Vries, A. (1977). *Mol. Cryst. Liq. Cryst.*, *41*, 27.

[4] De Vries, A., Ekachai, A., & Spielberg, N. (1979). *Mol. Cryst. Liq. Cryst. Lett*, *49*, 143.

[5] Hayashi, N., Kato, T., Fukuda, A., Vij, J. K., Panarin, Yu. P., Naciri, J., Shashidhar, R., Kawada S., & Kondoh, Sh. (2005). *Phys. Rev. E*, *71*, 041705.

[6] Bahr Ch., & Heppke, G., (1990). *Phys. Rev. A*, *41*, 4335.

[7] Manna, U., Song, J.-K., Panarin, Yu. P., Fukuda A., & Vij, J. K. (2008). *Phys. Rev. E*, *77*, 041707.

[8] Panarina, O. E., Panarin, Yu. P., Vij, J. K., Spector, M. S., & Shashidhar, R. (2003). *Phys. Rev. E*, *67*, 051709.

[9] Panarina, O., Panarin, Yu., Antonelli, F., Vij, J.K., Reihmann, M., Galli, G. (2006). *J. Mater. Chem.*, *16*, 842.

[10] Radcliffe, M. D., Brostrom, M. L., Epstein, K. A., Rappaport, A. G., Thomas, B. N., Shao, R. F., & Clark, N. A., (1999). *Liq. Cryst.*, *26*, 789.

[11] Lagerwall, S. T., Rudquist, P., & Giesselmann, F. (2009). *Mol. Cryst. Liq. Cryst.*, *510*, 148.

[12] Saunders, K. (2008). *Phys. Rev. E*, *77*, 061708 and (2009). *Phys. Rev. E, 80*, 011703.

[13] Gorkunov, M.V., Giesselmann, F., Lagerwall, J. P. F., Sluckin, T. J., & Osipov, M. A. (2007). *Phys. Rev. E*, *75*, 060701(R).

[14] Gorkunov, M. V., Osipov, M. A., Lagerwall, J. P. F., & Giesselmann, F. (2007). *Phys. Rev. E*, *76*, 051706.

[15] Xu, J., Selinger, R. L. B., Selinger, J. V., Ratna B. R., & Sashidhar, R. (1999). *Phys. Rev. E*, *60*, 5584.

[16] Spector, M. S., Heiney, P. A., Naciri, J., Weslowski, B. T., Holt, D. B., & Shashidhar, R. (2000). *Phys. Rev. E*, *61*, 1579.

[17] Selinger, J. V., Collings, P. J., & Shashidhar, R. (2001). *Phys. Rev. E*, *64*, 061705.

[18] Collings, P., Ratna B. R., & Shashidhar, R. (2003). *Phys. Rev. E*, *67*, 021705.

[19] Giesselmann, F., Zugenmaier, P., Dierking, I., Lagerwall, S. T., Stebler, B., Kaspar, M., Hamplova, V., & Glogarova, M. (1999). *Phys. Rev. E*, *60*, 598.

[20] Panov, V. P., Vij, J. K., Panarin, Yu. P., Blanc, C., Lorman V., & Goodby, J. W. (2007). *Phys. Rev. E*, *75*, 042701.

[21] Sandhya, K. L., Panarin, Yu. P., Panov, V. P., Vij, J. K., & Dabrowski, R. (2008). *Eur. Phys. J. E*, *27*, 397.

[22] Clark, N. A., Bellini, T., Shao, R.-F., Coleman, D., Bardon, S., Link, D. R., Maclennan, J. E., Chen, X.-H., Wand, M., D., Walba, D. M., Rudquist, P., & Largerwall, S. T. (2002). *Appl. Phys. Lett.*, *80*, 4097.

[23] Panarin, Yu. P., Kalinovskaya, O. E., Vij J. K., & Goodby, J. W. (1997). *Phys. Rev. E*, *55*, 4345.

[24] Panarin, Yu., Xu, H., Mac Lughadha, S. T., Vij, J. K., Seed, A. J., Hird, M., Goodby, J. W. (1995). *J. Phys.: Condens. Mater.*, *7*, L351.

[25] Panarina, O.E., Panarin, Yu., Antonelli, F., Vij, J. K., Reihmann, M., Galli, G. (2006). *J. Matter. Chem.*, *16*, 842.

[26] Manna, U., Song, J.-K., Panarin, Yu., Fukuda, A., Vij, J.K. (2006). *Phys. Rev. E*, *77*, 041707.

[27] Xu, H., Panarin, Yu., Vij, J. K., Seed, A., Hird, M., Goodby, J. W. (2008). *J. Phys.: Condens. Mater.*, *7*, 7443.